THE JOURNAL OF BIOLOGICAL CHEMISTRY VOL. 280, NO. 46, pp. 38416–38423, November 18, 2005

Adaptor Protein ARH Is Recruited to the Plasma Membrane by Low Density Lipoprotein (LDL) Binding and Modulates Endocytosis of the LDL/LDL Receptor Complex in Hepatocytes*

Received for publication, April 20, 2005, and in revised form, August 19, 2005 Published, JBC Papers in Press, August 29, 2005, DOI 10.1074/jbc.M504343200

Maria Isabella Sirinian[‡], Francesca Belleudi[§¶], Filomena Campagna[‡], Mara Ceridono[§], Tina Garofalo[§], Fabiana Quagliarini[‡§], Roberto Verna[§], Sebastiano Calandra[‖], Stefano Bertolini[**], Maurizio Sorice[§], Maria Rosaria Torrisi[§¶], and Marcello Arca[‡1]

*From the Departments of [‡]Clinical and Applied Medical Therapy and [§]Experimental Medicine and Pathology and [¶]Azienda Ospedaliera Sant'Andrea, University of Rome "La Sapienza," 00161 Rome, Italy, [‖]Department of Biomedical Sciences, University of Modena and Reggio Emilia, 41100 Modena, Italy, and **Department of Internal Medicine, University of Genoa, 16132 Genoa, Italy*

ARH is a newly discovered adaptor protein required for the efficient activity of low density lipoprotein receptor (LDLR) in selected tissues. Individuals lacking ARH have severe hypercholesterolemia due to an impaired hepatic clearance of LDL. It has been demonstrated that ARH is required for the efficient internalization of the LDL-LDLR complex and to stabilize the association of the receptor with LDL in Epstein-Barr virus-immortalized B lymphocytes. However, little information is available on the role of ARH in liver cells. Here we provide evidence that ARH is codistributed with LDLR on the basolateral area in confluent HepG2-polarized cells. This distribution is not modified by the overexpression of LDLR. Conversely, the activation of the LDLR-mediated endocytosis, but not the binding of LDL to LDLR, promotes a significant colocalization of ARH with LDL-LDLR complex that peaked at 2 min at 37 °C. To further assess the role of ARH in LDL-LDLR complex internalization, we depleted ARH protein using the RNA interference technique. Twenty-four hours after transfection with ARH-specific RNA interference, ARH protein was depleted in HepG2 cells by more than 70%. Quantitative immunofluorescence analysis revealed that the depletion of ARH caused about 80% reduction in LDL internalization. Moreover, our findings indicate that ARH is associated with other proteins of the endocytic machinery. We suggest that ARH is an endocytic sorting adaptor that actively participates in the internalization of the LDL-LDLR complex, possibly enhancing the efficiency of its packaging into the endocytic vesicles.

The low density lipoprotein receptor (LDLR)[2] plays a pivotal role in the regulation of cholesterol metabolism (1). LDLR is a ubiquitous cell surface glycoprotein of 839 amino acids that is able to bind low density lipoprotein (LDL), the major cholesterol transport vehicle in the plasma. The cellular and molecular biology of LDLR has been revealed through studies on familial hypercholesterolemia (FH) (1). FH is inherited as a co-dominant trait (2), and affected subjects show a markedly impaired LDLR function because of mutations in the LDLR gene (2). As a consequence, they present a decreased removal rate of circulating LDL and a dramatic increase in plasma cholesterol levels. Early studies on normal and FH fibroblasts demonstrated that LDLRs, shortly after being synthesized, appear on the cell surface where they gather in coated pits (1). These are specialized regions of cell membranes that are lined on the cytoplasmic surface by a protein called clathrin (3). After formation of the LDL-LDLR complex, the coated pits invaginate to form coated endocytic vesicles. Very quickly, the clathrin coat dissociates and multiple endocytic vesicles fuse to create endosomes (4–6). At the acid pH in endosomes, the LDL dissociates from the receptor, which returns to the surface to initiate another cycle of endocytosis (7, 8).

Recently, the identification of the molecular defect responsible for a recessive form of hypercholesterolemia that clinically resembles FH provided new insights into LDLR physiology. This disorder, called Autosomal Recessive Hypercholesterolemia (ARH), is caused by mutations in the putative adaptor protein ARH (9). *In vivo* studies demonstrated that ARH patients show a markedly reduced hepatic uptake of LDL similar to that found in homozygous FH (10).

ARH protein contains an ~130-residue phosphotyrosine-binding domain evolutionarily related to other adaptor proteins. Adaptor proteins containing phosphotyrosine-binding domains bind the conserved sequence motif NP*X*Y located in the cytoplasmic domain of various cell surface receptors and mediate several cellular functions, including receptor trafficking and endocytosis. The LDLR cytoplasmic tail contains a single NP*X*Y motif that is required for clustering and endocytosis of the receptor in fibroblasts. Point mutations in this highly conserved LDLR sequence eliminate binding of ARH to LDLR *in vitro*. The phosphotyrosine-binding sequence also binds inositol phospholipids, which may anchor the protein to the plasma membrane (11). The C-terminal portion of ARH protein contains a canonical clathrin box sequence (LLDLE in the human sequence) that binds the heavy chain of clathrin. ARH protein also has a highly conserved 27-amino acid sequence that binds the β_2 adaptin subunit of AP-2, which is a structural component of the clathrin-coated pits. On the basis of these data it has been proposed that ARH may function as a specific LDLR adaptor protein.

Elucidation of the specific role of ARH in the LDLR endocytosis has been hampered by the fact that cultured skin fibroblasts from ARH patients do not show major defects in LDL uptake and degradation (12).

* This work was supported by Telethon Grant GGP02149 and an Ateneo 2004 grant (to M. A.) and by grants from Ministero dell' Instruzione, Università e Ricera, from the Ministero della Salute, and from the Associazione Italiana per la Ricerca sul Cancro, Italy (to M. R. T.). The costs of publication of this article were defrayed in part by the payment of page charges. This article must therefore be hereby marked "*advertisement*" in accordance with 18 U.S.C. Section 1734 solely to indicate this fact.

[1] To whom correspondence should be addressed: Dipartimento di Clinica e Terapia Medica Applicata, Università di Roma "La Sapienza" Policlinico Umberto I, Viale del Policlinico 155, 00161 Rome, Italy. Tel.: 39-06-4450074; Fax: 39-06-4440290; E-mail: marcelloarca@libero.it.

[2] The abbreviations used are: LDLR, low density lipoprotein receptor; FH, familial hypercholesterolemia; ARH, autosomal recessive hypercholesterolemia; TRITC, tetramethylrhodamine isothiocyanate; siRNA, short interfering RNA; PBS, phosphate-buffered saline; FITC, fluorescein isothiocyanate.

Therefore, the majority of studies so far available have been carried out on lymphocytes from ARH patients, in which the LDLR function is significantly impaired (13, 14). It has been observed that the distribution of the immunodetectable LDLR is significantly altered in these cells and that it mostly resides on the plasma membrane. Moreover, although LDL degradation appears to be markedly reduced in lymphocytes, cell surface LDL binding is increased. This strongly indicates that ARH protein may be involved in the internalization of the LDL-LDLR complex (13).

How ARH works in hepatocytes is less known. It has been hypothesized that ARH may direct LDLR to the sinusoidal membrane. Experiments performed in ARH-deficient mice demonstrated that this was not the case. In *arh* −/− mouse livers, LDLR appears to be normally sorted to the sinusoidal surface (15). ARH might play a role in LDLR clustering, either by transporting the receptor to the coated pits or simply by anchoring the receptor in the pits (16). It must be noted, however, that LDLRs are dispersed on the plasma membrane of hepatocytes but clustered in coated pits on fibroblasts (17). Therefore, it is unlikely that an inappropriate anchorage of LDLR in coated pits is the major cause of LDLR malfunction in *arh*−/− hepatocytes. Moreover, immunoprecipitation experiments demonstrated that, at the steady state, the majority of ARH protein appears in fractions from which the LDLR receptor is absent (15), clearly indicating that ARH is not constitutively associated with the LDLR-clathrin complex. An alternative possibility is that the ARH protein is directly involved in the endocytic internalization of LDLR. We further investigated this possibility in the human hepatocyte cell line HepG2. To evaluate the consequence of the absence of ARH protein on LDLR trafficking we employed short interfering RNA (siRNA) methodology. This has been demonstrated to be the most powerful way to selectively reduce the intracellular concentration of proteins (18, 19). The siRNA-transfected cells were examined by immunofluorescence, Western blotting, and functional endocytosis assay. Our results indicate that ARH is not constitutively associated with LDLR at the plasma membrane; instead, ARH is mainly recruited to the membrane after LDL binding, thus facilitating the endocytosis of the LDL-LDLR complex. Collectively, our data provide evidence that the ARH protein is an important component of the endocytic machinery of LDLR in hepatocytes.

MATERIALS AND METHODS

Reagents—Enhanced chemiluminescence (ECL) Western blotting detection reagents, Hybond ECL nitrocellulose membrane, and Protein G/Protein A-Sepharose 4 Fast-Flow beads were from Amersham Biosciences. Protease inhibitor mixture tablets with and without EDTA were purchased from Roche Diagnostics. Laemmli sample buffer and phosphate-buffered saline with Tween 20 (PBST, pH 7.4) were obtained from Sigma. Transfections were done with a TransMessenger transfection kit from Qiagen GmbH (Hilden, Germany). A Bio-Rad protein assay kit was purchased from Bio-Rad Diagnostics.

Antibodies—Rabbit polyclonal antibodies against Rab-4 (D-20) and anti-lysosome-associated membrane glycoprotein (LAMP-1) (H-228), anti-early endosomal antigen 1 (EEA1), goat polyclonal antibodies against β-adaptin (N-19), Dab2 (C-20), and clathrin heavy chain (C-20) were purchased from Santa Cruz Biotechnology (Santa Cruz, CA). Rabbit polyclonal antibodies against ARH and LDLR were a kind gift from Dr. H. H. Hobbs (University of Texas Southwestern Medical Center, Dallas, TX). Mouse monoclonal antibody against LDLR (Ab-1) was purchased from Oncogene Research Products (Boston, MA). Horseradish peroxidase-conjugated anti-mouse or anti-rabbit secondary antibodies were from Amersham Biosciences. Horseradish peroxidase-conjugated goat antibody and rabbit polyclonal antibody against actin were from Sigma.

Cell Culture—Human HepG2 cells (obtained from ATCC) were cultured in Dulbecco's modified Eagle's medium supplemented with 10% fetal bovine serum plus antibiotics (Sigma). To reach different levels of confluence, HepG2 cells were plated on round glass coverslips coated with 2% gelatin (Sigma) at a density of 1×10^5 cells. To ensure that bile canaliculus-like regions were formed *de novo* during the culture period, cells were vigorously separated before plating. Cells were allowed to grow for 72 h to obtain confluent polarized cells. After this culture period, HepG2 cells develop bile canaliculus-like structures (BC) located between adjacent cells at the apical pole of the cell (20). The plasma membrane of BC has many microvilli that contain high concentrations of F-actin (21).

Sucrose Gradients—HepG2 cells were cultured as described above. Sucrose gradient fractions were obtained according to Stockinger *et al.* (22). Briefly, confluent dishes were serum starved for 16 h, kept on ice, and suspended in 300 μl of buffer (3 mM imidazole, pH 7.4, 1 μM EDTA, Sigma protease inhibitor mixture) containing 8.5% sucrose. Cells were disrupted by 20 strokes in a Dounce homogenizer, and the efficiency was monitored by microscopy (Olympus Italia, Segrate, Milan, Italy). Nuclei were removed by 10 min of centrifugation at $1000 \times g$, and the supernatant was loaded on top of 4 ml of a 10–40% continuous sucrose gradient and spun for 16 h in a Beckman ultracentrifuge (swinging bucket rotor, SW60 Ti) at 40,000 rpm. Fractions (200 μl) were collected from the bottom of the tube by puncturing with an 18-gauge needle and analyzed by Western blotting using anti-ARH polyclonal antibody and anti-LDLR monoclonal antibody (Ab-1) as well as anti-LAMP-1, anti-EEA1, or anti-Rab-4 polyclonal antibodies.

Short Interfering RNA—21-nucleotide RNA duplexes with symmetric 2-nucleotide 3′(2′-deoxy) thymidine overhangs (corresponding to the ARH gene nucleotides 88–112 relative to the start codon) were purchased from Xeragon (Zurich, Switzerland). RNA sequences were: sense, 5′-GCUGCCUGAGAACUGGACAdTdT-3′; antisense, 5′-UGUCCAGUUCUCAGGCAGCdTdT-3′. Selected sequences were submitted to BLAST searches against the human genome sequence to ensure that only the desired mRNA was targeted. The silencing efficiency of selected siRNAs was first tested in cell culture experiments. The experimental conditions were as follows: to obtain 50–80% confluence in 24 h, about 2×10^5 cells/well were seeded in 12-well plates on the day before transfection. On the day of transfection, the cells were washed with PBS and then each well received 600 μl of RPMI 1640 growth medium containing 200 μl of buffer EC-R, 1.6 μg of siRNA, 3.2 μl of Enhancer R, and 8 μl of TransMessenger prepared following the TransMessenger kit directions. After 3 h of incubation at 37 °C, cells were washed and normal growth medium (1 ml) was added. After 24 and 48 h, Western blot analysis of ARH was carried out. siRNA-treated cells were trypsin digested in 12-well plates at 37 °C until the cells detached. The cells were washed twice with PBS and then lysed in lysis buffer (1% Triton, 50 mM Tris, pH 8.0, 2 mM $CaCl_2$, 80 mM NaCl) supplemented with protease inhibitors. Total protein content of cell lysates was determined by Bio-Rad protein assay. Lysate volumes containing comparable amounts of total proteins were used for Western blotting.

Western Blotting—Lysate samples were boiled for 5 min in Laemmli sample buffer (4% SDS, 20% glycerol, 10% 2-mercaptoethanol, 0.004% bromphenol blue, and 0.125 M Tris-HCl, pH 6.8) and separated by SDS-PAGE on 10% running gels. The proteins were transferred to Hybond ECL nitrocellulose membranes that had been blocked for 1 h at 37 °C with PBST containing 5% dry milk and 5% calf serum. The membranes

were then incubated for 1 h at 37 °C with primary antibodies, followed by horseradish peroxidase-conjugated secondary antibody and detection by ECL.

Co-immunoprecipitation—HepG2 cells (5×10^6 cells) were seeded in 100-mm dishes and grown for 2 days to reach confluence. Cells were serum starved for 16 h and kept on ice for 30 min. Purified LDL (50–100 μg) was added, and the cells were left for 1 h at 4 °C and then incubated at 37 °C for an additional 2, 3, 5, or 10 min before lysis. Cells were scraped with 1 ml of incubation buffer (5 mM Tris, pH 7.5, 100 mM NaCl, 2 mM $CaCl_2$, 2 mM $MgCl_2$) in the presence of protease inhibitors without EDTA and lysed by sonication for 5 s at room temperature. As a control, HepG2 cells were serum starved for 16 h and immediately lysed; in addition, one 100-mm dish was serum starved for 16 h, incubated at 4 °C for 1 h with purified LDL, and lysed. The amounts of protein in the lysates were estimated by spectrophotometry, and concentrations were normalized by addition of buffer. Lysates (an estimated 500 μg of protein) were incubated with 25 μl of Protein G/Protein A-Sepharose beads in 25 μl of incubation buffer for 1 h. The beads were removed by centrifugation, and the supernatants were incubated with anti-Rab-4, anti-clathrin, and anti-β-adaptin at 4 °C overnight. The antibody complexes were captured by addition of 25 μl of Protein G/Protein A-Sepharose beads in 25 μl of incubation buffer and a 1-h incubation at 4 °C in a rotating shaker. Bead-bound immune complexes were washed twice with incubation buffer, collected by centrifugation, resuspended in 30 μl of Laemmli sample buffer, and visualized by SDS-PAGE and Western blotting.

Microinjection—siRNA (100 nM in 1 ml of PBS buffer containing dextran-FITC at 1 mg/ml) or buffer with dextran-FITC alone as a control were microinjected into the cytoplasm of HepG2 cells to induce RNA interference and consequent ARH silencing (23). Microinjection was performed using an Eppendorf microinjector (Eppendorf, Hamburg, Germany) and an inverted microscope (Zeiss, Oberkochen, Germany). Injection pressure was set at 30–80 hPa and the injection time at 0.3–0.5 s. Microinjected cells were left for 8 h at 37 °C, serum starved for 16 h, and then treated with the fluorescent conjugate DiI-LDL (Molecular Probes, Eugene, OR) as below.

Functional Assay of LDLR—The function of LDLR was tested by using Dil-LDL or anti-LDLR C7 monoclonal antibody. For DiI-LDL treatment, confluent polarized HepG2 cells were serum starved for 16 h, washed with medium, treated with medium containing 5 μg/ml DiI-LDL or anti-LDLR C7 antibody for 5 min at 37 °C to induce LDLR internalization, and immediately fixed with 4% p-formaldehyde in PBS for 30 min. Alternatively, cells serum starved for 16 h were washed with cold medium, incubated with medium containing 5 μg/ml DiI-LDL for 1 h at 4 °C, and either immediately fixed or washed with prewarmed medium and incubated at 37 °C for an additional 2, 5, and 10 min before fixation.

Immunofluorescence Microscopy—For conventional immunofluorescence, cells grown on coverslips were fixed with 4% p-formaldehyde in PBS for 30 min at 25 °C and permeabilized with 0.1% Triton X-100 for 5 min. In double immunofluorescence experiments, cells were incubated with anti-ARH polyclonal antibody (1:50 in PBS) and anti-LDLR monoclonal antibody (1:100 in PBS). The primary antibodies were visualized using FITC-conjugated goat anti-rabbit IgG (1:300 in PBS; Cappel Research Products, Durham, NC), Texas Red-conjugated goat anti-rabbit IgG (1:100 in PBS; Jackson Immunoresearch Laboratories Inc., West Grove, PA), or Texas Red-conjugated goat anti-mouse IgG (1:100 in PBS; Jackson Immunoresearch Laboratories). F-actin in microvilli of bile canaliculus was stained with TRITC-conjugated phalloidin (TRITC-Ph) (1:50 in PBS; Sigma) for 45 min at 25 °C. Fluorescent images were recorded and analyzed using a cooled CCD color digital camera SPOT-2 (Diagnostic Instruments Inc., Milan, Italy) and FISH 2000/H1 software (Delta Sistemi, Rome, Italy). Colocalization of the fluorescence signals was evaluated using a Zeiss confocal laser scan microscope (Zeiss, Oberkochen, Germany). To prevent cross-talk between the two signals, the multitrack function was used. Quantitative analysis of the DiI-LDL internalization in uninjected or injected cells was performed evaluating five different areas of each slide randomly taken from three different experiments; results are expressed as percentage of cells presenting internalized DiI-LDL.

RESULTS

The Intracellular Localization of ARH Protein Is Related to Cell Polarity—To analyze ARH expression and distribution in human hepatocytes, we investigated the intracellular localization of ARH protein and the possible colocalization with LDLR in HepG2 cells, a hepatoma cell line that grows to subconfluent monolayers in 12 h or to confluent polarized monolayers in 72 h. As previously described for primary cultured fibroblasts and the HeLa epithelial cell line (11), we found that in non-confluent, non-polarized HepG2 cells the ARH signal appears punctate and homogenously dispersed throughout the cytoplasm (Fig. 1*A*). In confluent HepG2 monolayers, the cells are polarized and form distinct bile canaliculus-like structures that contain a well organized actin cytoskeleton and can be intensely stained with TRITC-phalloidin (21). The ARH signal in these cells is also punctate but prevalently distributed in the basolateral regions, and to a lesser extent evident in the proximity of the apical poles (Fig. 1*B*, *arrow*).

To compare the localization of ARH and LDLR, we performed double immunofluorescence experiments in confluent, polarized cells using anti-ARH polyclonal antibody and anti-LDLR monoclonal antibody. In this experiment, ARH appeared to be colocalized with the receptor in the basolateral area of the cells (Fig. 1*C*).

Activation of LDLR Promotes ARH Recruitment to Plasma Membrane—We then investigated the ARH and LDLR localization after the up-regulation of LDLR expression by serum starvation for 16 h. Although these conditions increase the presence of receptors on the cell surface, they did not modify the ARH and/or LDLR distribution or induce a colocalization of ARH with LDLRs on the plasma membrane (Fig. 2*A*).

To determine whether ARH distribution is affected by binding of LDL to LDLR, we serum starved HepG2 cells for 16 h and then treated them with DiI-LDL for 5 min at 37 °C before fixation. Double immunofluorescence with anti-ARH polyclonal antibodies showed that ARH and DiI-LDL colocalized at the plasma membrane (Fig. 2*B*), suggesting that ARH could be partially recruited to the plasma membrane after LDL binding to the LDLR. To further explore whether the ARH recruitment might be the direct result of ligand binding to the receptor or due to lipid transfer, we performed additional experiments in which the LDLR pathway was activated by addition of anti-LDLR C7, an antibody directed against the extracellular portion of the LDLR. Anti-LDLR C7 is known to induce internalization and recycling of LDLR similarly to LDL particles (24). Double immunofluorescence with anti-ARH polyclonal antibodies showed that ARH protein partially colocalizes with LDLR-anti-LDLR complexes (Fig. 2*C*).

As noted in the Introduction, LDLR tends to cluster in clathrin-coated pits on the cell surface under defined conditions. Low temperature permits LDL binding to LDLR on the plasma membrane but inhibits the clustering in clathrin-coated pits of LDL-LDLR complexes. Subsequent warming to 37 °C induces a synchronous wave of endocytosis, with a massive clustering of LDL-LDLR complexes in the clathrin-

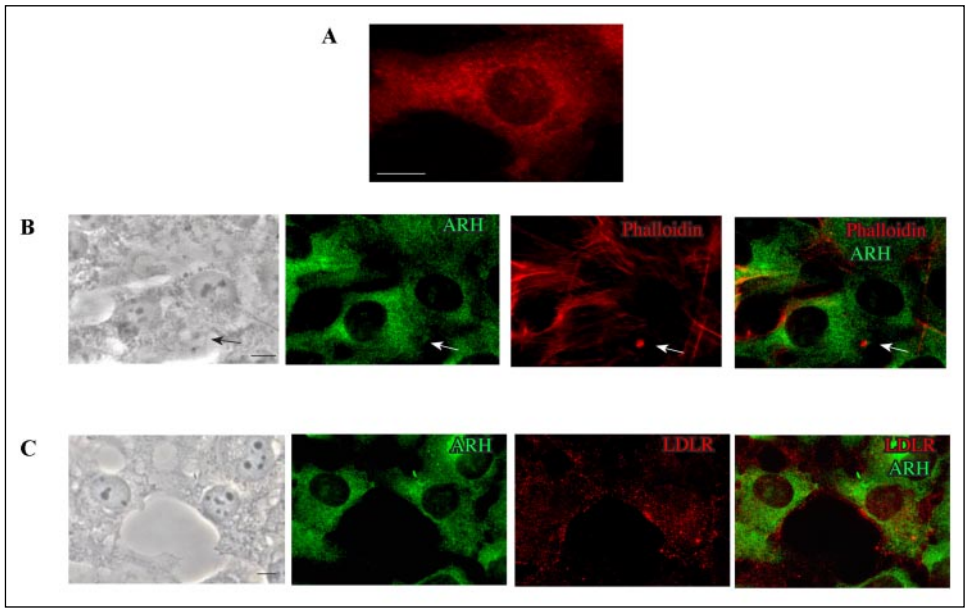

FIGURE 1. **Immunofluorescence analysis of the intracellular localization of ARH protein.** *A*, subconfluent HepG2 cells were fixed and labeled with anti-ARH polyclonal antibody; the ARH signal is punctate and sparse all over the cell cytoplasm. *B*, confluent, polarized HepG2 cells were fixed and double labeled with anti-ARH polyclonal antibodies and phalloidin-TRITC; the ARH punctate signal (*green*) is mainly distributed in the basolateral region of the cells and is less evident in the proximity of the bile canalicular apical region identified by phalloidin-TRITC-positive (*red*) dots (*arrow*). *C*, double immunolabeling with anti-ARH polyclonal antibodies and anti-LDLR monoclonal antibody shows codistribution of ARH protein (*green*) and LDLR (*red*) on the same basolateral region of the cell. *Bars*, 10 μm.

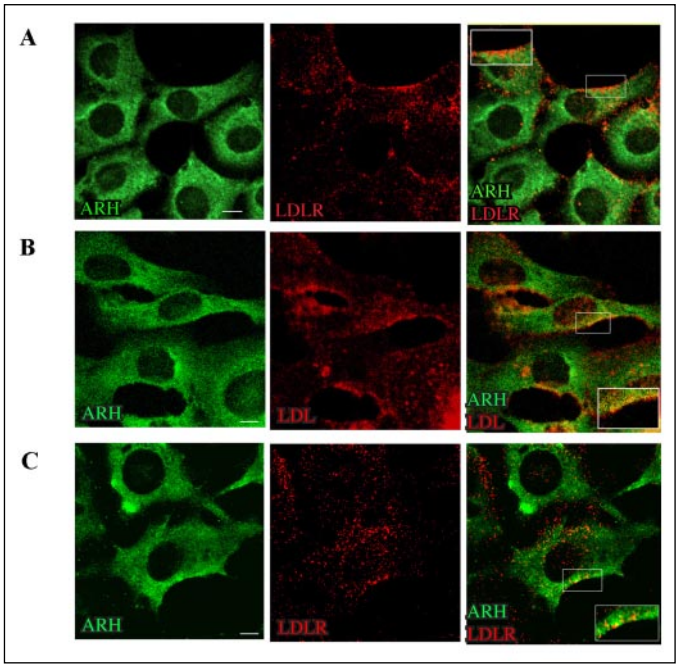

FIGURE 2. **Confocal analysis of the colocalization of ARH with LDLR induced by LDL binding to the receptor.** *A*, confluent polarized HepG2 cells were serum starved for 16 h, fixed, and double immunolabeled with anti-ARH polyclonal and anti-LDLR monoclonal antibodies. The confocal analysis reveals that the up-regulation of LDLR induced by serum starvation does not modify ARH (*green*) and/or LDLR (*red*) distribution and that ARH protein does not appear to colocalize with LDLR on the plasma membrane. *B*, confluent polarized HepG2 cells were serum starved for 16 h and treated with DiI-LDL for 5 min at 37 °C. Immunolabeling with anti-ARH polyclonal antibody and subsequent confocal analysis reveals that, after LDL treatment, ARH protein (*green*) and DiI-LDL-LDLR complexes (*red*) colocalize on the plasma membrane. The extent of colocalization is shown in *yellow* after merging. *C*, confluent polarized HepG2 cells were serum starved as above and treated with anti-LDLR C7 monoclonal antibody for 5 min at 37 °C. Double immunofluorescence with anti-ARH antibody and anti-LDLR and confocal analysis reveals that ARH protein (*green*) and anti-LDLR bound to the receptor (*red*) colocalize on the plasma membrane. Colocalization is shown in *yellow* after merging. *Bars*, 10 μm.

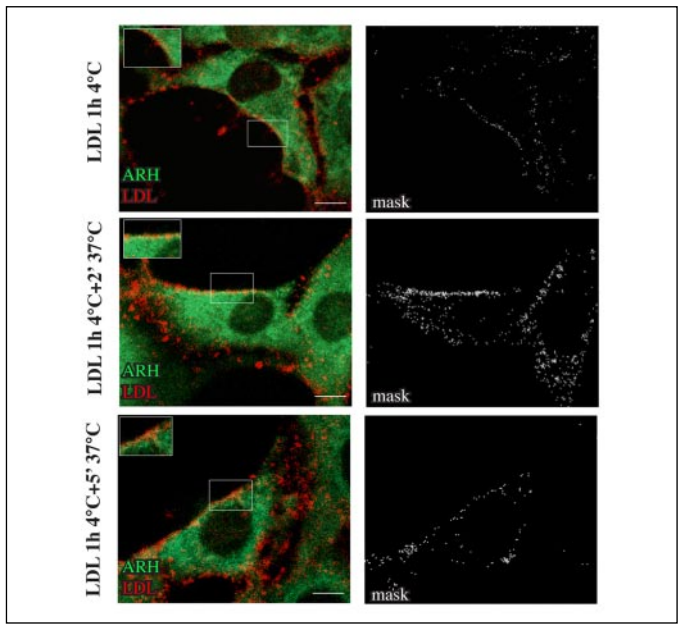

FIGURE 3. **Confocal analysis of the colocalization of ARH with LDL during ligand-receptor clustering in clathrin-coated pits.** Confluent polarized HepG2 cells were serum starved for 16 h, treated with DiI-LDL for 1 h at 4 °C, and warmed to 37 °C for 2 and 5 min. Immunolabeling with anti-ARH polyclonal antibodies and subsequent confocal analysis reveals that ARH protein (*green*) and DiI-LDL-LDLR complexes (*red*) colocalize only slightly at 4 °C, whereas colocalization of the two signals at the cell plasma membrane appears evident after warming to 37 °C for 2′. At 5′ time point of warming, the extent of colocalization decreases, although it is still evident at the cell surface as well as in intracellular dots. The extent of colocalization is shown in *yellow* after merging and as *white dots* in masked images.

coated pits. To discriminate whether the recruitment of ARH to the cell surface was dependent on the binding of LDL to LDLR or on the LDL-LDLR clustering in the clathrin-coated pits, we serum starved HepG2 cells for 16 h as above, treated them with DiI-LDL for 1 h at 4 °C, and then warmed the cells to 37 °C for different times. Double immunofluorescence and subsequent confocal analysis showed that, after treatment at low temperature, ARH colocalized only weakly with DiI-LDL distributed on the plasma membrane (Fig. 3). In fact, colocalization of ARH with fluorescent LDL at the level of the plasma membrane appeared maximal after 2 min at 37 °C (Fig. 3) and rapidly decreased, although it was still evident after 5 min (Fig. 3) when LDL appeared also in intracellular endocytic dots. These results indicate that ARH could be involved in the early steps of LDLR endocytosis. Very weak ARH/LDL colocalization after treatment with the ligand at low temperature and

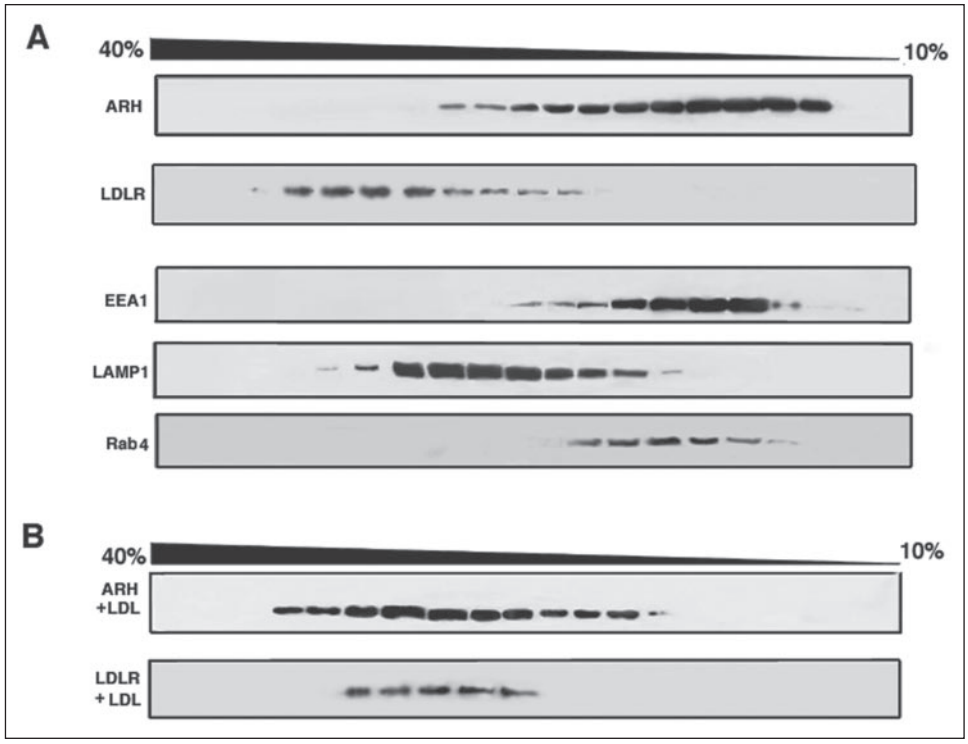

FIGURE 4. **Sucrose gradient analysis of the localization of ARH and LDLR.** Cells were harvested and postnuclear supernatant prepared and loaded on top of a 10–40% continuous sucrose gradient as described under "Materials and Methods." After centrifugation, fractions were collected, and samples (30 μl) of each fraction were separated by SDS-PAGE and analyzed by Western blot using antibodies against ARH, LDLR, EEA1, Lamp-1, and Rab-4. After LDL treatment (2 min) ARH is shifted toward higher densities where LDLR is localized.

the maximal ARH/LDL overlap at very early time points of warming to 37 °C strongly suggest that ARH protein could play a role in the recruitment of LDL-LDLR complexes in clathrin-coated pits (Fig. 3).

We also attempted to analyze the relative distribution of ARH and the LDLR within the various endocytic compartments in cells before and after stimulation of LDLR pathway by adding LDL. Analytical centrifugation was performed to fractionate vesicles from HepG2 cells on a continuous sucrose gradient (Fig. 4). LAMP-1, EEA1, and Rab-4 antibodies were also used in Western blot analyses to determine the position of endocytic structures. As previously reported (15), in control untreated cells the majority of ARH co-sedimented with vesicles containing EEA1 and Rab-4 (Fig. 4*A*). Only a small percentage of ARH was present in the same fractions as the LDLR (Fig. 4*A*). Conversely, 2 min after LDL addition, ARH distribution showed a marked shift toward higher density fractions where LDLR was mainly localized (Fig. 4*B*). These findings are consistent with ARH being recruited to LDLR-containing early endocytic vesicles when LDLR internalization is stimulated.

To provide a more direct confirmation of immunofluorescence as well as subcellular fractionation experiments, we evaluated the association of ARH with LDL-LDLR complexes in clathrin-coated pits at different times of incubation with LDL (Fig. 5). Cell-free lysates were immunoprecipitated using the anti-clathrin monoclonal antibody followed by Protein G/Protein A-Sepharose beads. Western blot analysis using the anti-ARH antibody revealed a positive band in samples treated with LDL for 2 min. The band was still evident after 5 min of treatment and declined thereafter. As expected, no association was found in control untreated cells. These findings further indicate that ARH could be partially recruited to the plasma membrane during early steps of LDLR-mediated endocytosis.

Silencing of ARH Is Able to Block LDL-LDLR Endocytosis—To determine the involvement of ARH in binding of the LDL-LDLR complex to the clathrin-coated pits, we inhibited the expression of the ARH protein in the human hepatic HepG2 cell line using an siRNA duplex that targeted the segment 88–112 of the ARH open reading frame (Fig. 6*A*).

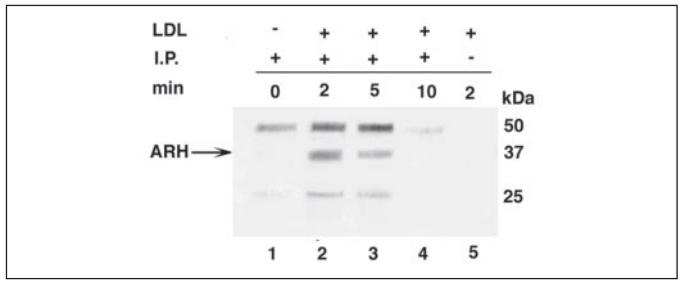

FIGURE 5. **ARH co-immunoprecipitates with clathrin after LDL treatment.** HepG2 cells were lysed and immunoprecipitated with anti-clathrin antibody, and the precipitated proteins were separated by 10% SDS-PAGE and immunoblotted with anti-ARH antiserum (1:1000) as described under "Materials and Methods." The immunoprecipitation assay was carried out at different times of LDL incubation. *Lane 1*, control untreated cells immunoprecipitated with anti-clathrin antibody; *lane 2*, cells treated with LDL for 2 min and immunoprecipitated with anti-clathrin antibody; *lane 3*, cells treated with LDL for 5 min and immunoprecipitated with anti-clathrin antibody; *lane 4*, cells treated with LDL for 10 min and immunoprecipitated with anti-clathrin antibody; *lane 5*, cells treated with LDL for 2 min and immunoprecipitated with a nonspecific IgG antibody. ARH associates with clathrin after 2 and 5 min of LDL treatment.

This strategy could mimic the *in vivo* pathological loss of function of the hepatic LDL uptake in ARH patients. Cells were transfected with siRNA, or with duplex of unrelated scrambled sequence as a positive control, or with transfection reagent alone as negative control. To quantitate the reduction of ARH expression, the cells were lysed 24, 48, and 72 h after transfection and analyzed by immunoblotting with anti-ARH or anti-actin antibodies as a control (Fig. 6*B*). Twenty-four hours after the transfection, the amounts of ARH protein were strongly reduced (~70–80% decrease), whereas the amount of actin had changed only slightly. The lysates obtained 48 h after incubation with siRNA showed a slight increase of ARH, and this was more evident 72 h after transfection. This may have been due to the growth of cells transfected poorly or not at all.

HepG2 cells were microinjected with a mixture of siRNA for ARH and dextran-FITC to identify injected cells or with dextran-FITC alone as a control. After microinjection, cells were left at 37 °C for 8 h and

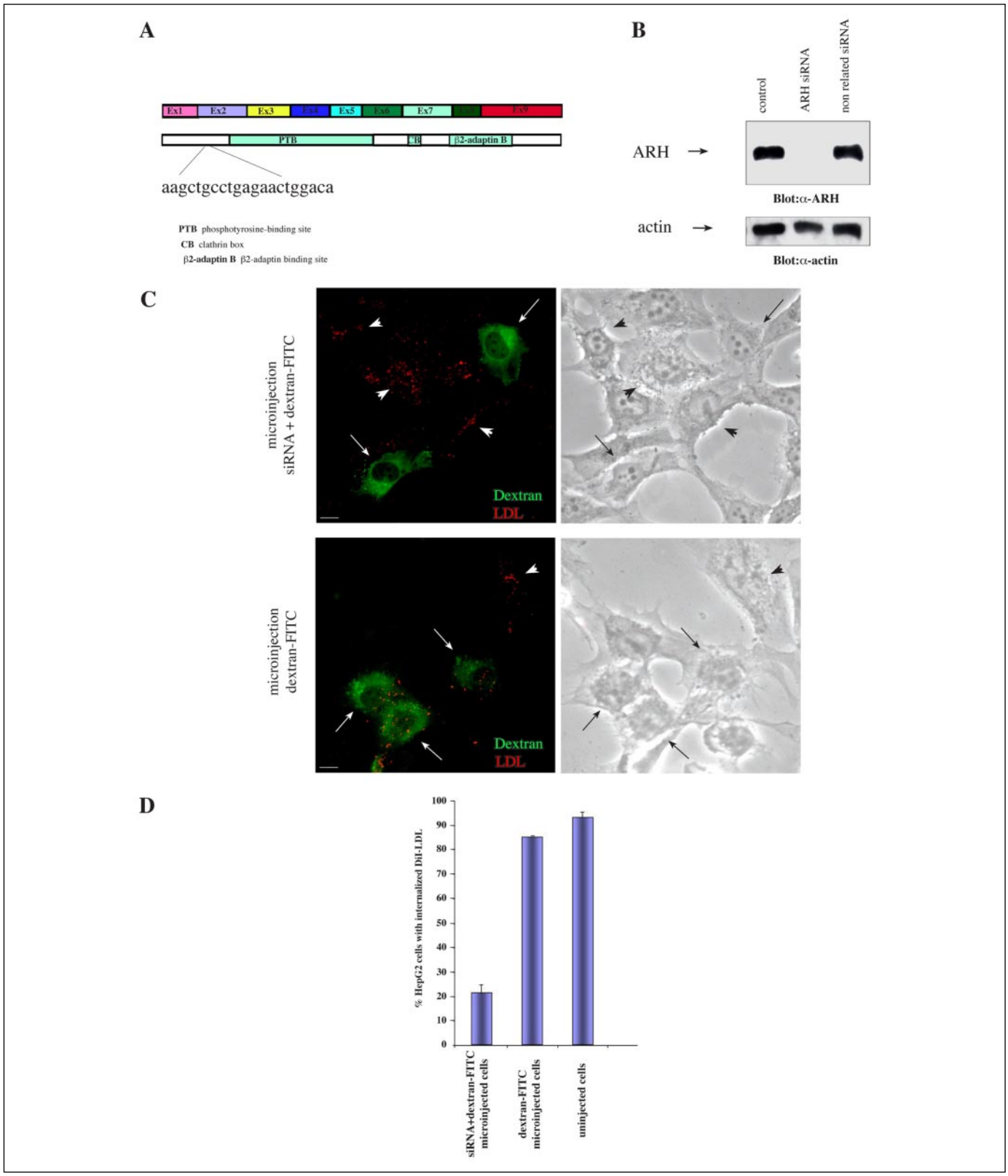

FIGURE 6. **Effect of the microinjection of siRNA for ARH on LDL internalization.** *A*, sequence of the siRNA used for the microinjection experiments. *B*, effect of the transfection of siRNA for ARH on the ARH protein expression in HepG2 cells. HepG2 cells were transfected with the siRNA for ARH or with a non-related siRNA. After 24 h, ARH protein expression was evaluated by Western blot using anti-ARH polyclonal antibodies. Approximately equal protein loading of the gel was verified using an anti-actin antibody. *Lane 2*, HepG2 transfected with ARH siRNA; *lane 3*, control HepG2 transfected with a non-silencing RNA sequence (fluorescein-labeled duplex siRNA); *lane 1*, negative control. *C*, confluent polarized HepG2 cells were microinjected with a mixture of Dextran-FITC and siRNA for ARH and/or with Dextran-FITC alone as a control. After microinjection, cells were incubated at 37 °C for 24 h and then treated with Dil-LDL for 10 min at 37 °C before fixation. Immunofluorescence analysis shows that in cells injected with siRNA for ARH (*arrows*), Dil-LDL internalization is blocked, whereas in uninjected cells (*arrowheads*) or in cells injected with dextran-FITC alone (*arrows*), Dil-LDL internalization appears to be unmodified, and the ligand appears concentrated in the intracellular endocytic dots. *D*, quantitative analysis of Dil-LDL internalization expressed as percentage of cells presenting internalized Dil-LDL. A total of 100 cells microinjected with siRNA for ARH and dextran-FITC or with Dextran-FITC alone were compared with uninjected cells. Results represent the mean values ± one S.D. from three different experiments. *Bars*, 10 μm.

serum starved for an additional 16 h. At 24 h after microinjection, cells were treated with DiI-LDL for 10 min at 37 °C and then fixed for microscopy. In uninjected cells and cells injected only with dextran-FITC as a control, DiI-LDL was concentrated in intracellular endocytic dots, whereas in cells microinjected with siRNA and dextran-FITC mixture no intracellular LDL-positive dots were visible (Fig. 4*C*). Thus, the silencing of ARH was sufficient to functionally block DiI-LDL internalization. This suggests that, at least in HepG2 cells, ARH protein plays an essential role in the LDLR endocytic process. Quantitative analysis performed by counting uninjected or injected cells presenting internalized LDL in five different areas of each slide randomly taken from three different experiments revealed that the inhibition of LDL endocytosis was evident in 80% of the cells injected with siRNA (Fig. 4*D*).

Interaction of ARH with Endocytic Proteins in Polarized HepG2 Cells—To demonstrate interaction of ARH with other proteins involved in the clathrin-mediated internalization process *in vivo*, we carried out immunoprecipitations with anti-β-adaptin, anti-Dab2, and anti-Rab-4 followed by immunoblotting for ARH. All experiments were carried out at baseline and after stimulating the endocytic pathway by addition of purified LDL to the cell culture medium (Fig. 7). As already reported in the literature (14), we observed co-immunoprecipitation of the ARH protein with several components of the plasma membrane endocytic system, including the β subunit of the AP-2 complex (β-adaptin) and the Dab2 protein. In addition, we observed co-immunoprecipitation of ARH with the small GTPase Rab-4, which is a component of the early endosome and recycling arms of the endocytic pathway. It is interesting to note that the pattern of co-immunoprecipitation of ARH with β-adaptin, Dab2, and Rab-4 was already present at 4 °C and was not apparently modified at later times after LDL addition.

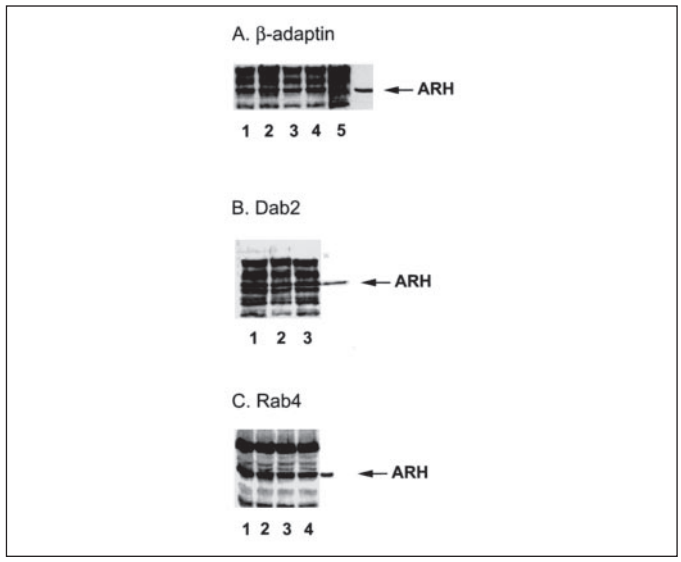

FIGURE 7. **β-Adaptin, Dab2, and Rab-4 co-immunoprecipite with ARH.** After 1 h of incubation with LDL at 4 °C, HepG2 cells were lysed and immunoprecipitated with the specific antibody, and the precipitated proteins were separated by 10% SDS-PAGE and immunoblotted with anti-ARH antiserum (1:1000) as described under "Materials and Methods." The immunoprecipitation assay was carried out at different times of LDL incubation: *lane 1* corresponds to 1 h of incubation with LDL at 4 °C, and *lanes 2*, *3*, and *4* correspond to immunoprecipitation carried out after 2, 5, and 10 min of incubation with LDL at 37 °C, respectively. *Lane 5* is a negative control experiment where 25 μl of Protein G/Protein A-Sepharose beads were incubated with anti-β-adaptin at 4 °C overnight without cell lysate.

DISCUSSION

The results of this study demonstrate that the adaptor protein ARH plays a crucial role in the internalization of LDLR by hepatocytes. Transient loss of ARH by siRNA resulted in the failure of LDL endocytosis and the almost complete absence of the LDL-LDLR complex in the internal compartment of hepatocytes. In fact, the immunofluorescence analysis revealed that in hepatocytes lacking ARH, most of the LDL resides on the cell surface.

The role of ARH in LDLR function has been extensively investigated in circulating lymphocytes based on the fact that transformed lymphocytes and monocyte-derived macrophages obtained from ARH patients are unable to take up and degrade ^{125}I-LDL (13, 25, 26). The results of these studies clearly suggested that ARH is required for the efficient endocytosis of LDLR in these cells. More recently, it has been observed that lymphocytes obtained from ARH-negative patients did not accumulate LDL-gold complex in multivesicular bodies characteristic of late endosomes and lysosomes, thus confirming the lack of internalization of LDL in these cells (27). Less information is available on the role of ARH in LDLR function in liver cells. In a recent study, Harada-Shiba *et al.* (28) observed that after *in vivo* injection of [^{3}H]cholesteryl oleyl ether-labeled LDL, less radioactivity is recovered from the liver of ARH-deficient mice than from livers of wild-type mice. Surprisingly, the same authors reported that uptakes of [^{3}H]cholesteryl oleyl ether-labeled LDL, ^{125}I-LDL, and Dil-LDL were all normal when *arh*−/− hepatocytes were cultured. This is in contrast with our finding that the loss of ARH arrested the LDLR trafficking cycle at the point of endocytosis from the cell surface in HepG2 cells. On the other hand, our observations concur with the evidence that hepatic clearance of LDL from plasma is markedly retarded in *arh*−/− mice as well as in ARH patients (12, 15).

Several hypotheses have been proposed to explain how ARH might be involved in the endocytosis of LDL-LDLR complex. One is that ARH acts by facilitating the interaction between the cytoplasmic tail of LDLR and some structural components of the coated pits, such as the AP2 protein and the clathrin heavy chain. This is mainly based on the observation that ARH protein can bind to LDLR, clathrin, and AP-2 (14). However, some of our evidence contradicts this hypothesis. In particular, we observed that the majority of ARH protein in hepatocytes appears in fractions where the LDLR receptor is absent, clearly indicating that ARH is not constitutively associated with the LDLR-clathrin complex (15). The second major finding from our study is that ARH protein is recruited to plasma membrane after stimulation of LDL internalization. In fact, we observed by immunofluorescence that the overlap of ARH protein with the LDL-LDLR complex at the level of the plasma membrane was almost negligible at 4 °C but became significant at 37 °C. After 10 min, when LDL appeared exclusively in intracellular endocytic dots, no more ARH protein could be colocalized with the LDL-LDLR complex. These findings were corroborated by our subcellular fractionation and immunoprecipitation time course experiments, in which clathrin-associated LDL-LDLR complexes showed co-immunoprecipitation with ARH transiently 2–5 min after the LDLR pathway was activated. Those results indicated that ARH is recruited to LDLR-containing early endocytic compartments. Our result is consistent with the report by Mishra *et al.* (11) that ARH associates with the LDLR during the early stages of endocytosis in HeLa cells. Moreover, Mishra *et al.* suggested that the kinetics of intracellular juxtaposition of LDLR and ARH are consistent with those occurring within the clathrin-coated buds and/or vesicles. On the other hand, they also documented (11) that ARH protein is not enriched in liver or in brain clathrin-coated vesicles, as one might expect if this protein were a constitutive part of the clathrin-coated pit machinery. Conversely, their observations favor the hypothesis that ARH may be an endocytic sorting adaptor that could actively participate in the sorting of endocytic cargo but does not progress with it into the budded vesicles. There are several examples of

mechanisms like this, including eps15 and epsin (29). Another interesting question is whether ARH recruitment is due to lipid transfer or is the direct result of ligand binding to the LDLR. Our immunofluorescent experiments carried out using anti-LDLR C7, a non-physiological ligand containing neither apolipoprotein B nor lipids, clearly suggest that the activation of LDL internalization is the signal that induces movement and recruitment of ARH.

Clathrin-coated vesicles move cell surface receptors to the endosomes. Some of these endosomes are recycled, that is, returned to the plasma membrane (30). Principal structural components of plasma membrane-derived clathrin-coated vesicles are clathrin and the heterotetrameric adaptor protein AP-2. In addition to adaptors, a number of accessory proteins are involved in the clathrin-coated vesicle assembling and movement. To explore the interactions between ARH with other endocytic proteins, we carried out several co-immunoprecipitations experiments before and after addition of LDL to the cell culture medium. We found that ARH is associated with β-adaptin and Dab2, in agreement with similar findings by Mishra *et al.* (11). In addition, we observed that Rab-4 may colocalize with ARH. We were unable to detect any kinetics in these associations. This may be due either to the limited sensitivity of our semiquantitative Western blotting or to difficulty in establishing the stoichiometry of ARH complexes with these proteins. Stable transfection of HepG2 with anti-ARH siRNA might allow clarification of these aspects. In this regard, Jones *et al.* (15) reported that at steady state ARH co-sediments with Rab-5 and EEA1, both markers of the early endosomal compartment. These observations strongly suggest that ARH may associate with endocytic accessory proteins of the early endosome compartment. Association of ARH with Rab-4 is particularly interesting, because Rab-4 is a component of the early endosome compartment and it also participates in the recycling arms of the endocytic pathway (31, 32). Therefore, it can be hypothesized that ARH is allowed to enter into another cycle of endocytosis through its association with Rab-4. Further studies are needed to better clarify the relationship between ARH and the other endocytic accessory proteins.

In summary, our findings demonstrate that ARH protein is required to promote the internalization of the LDL-LDLR complex into hepatocytes. At steady state, ARH appears to be colocalized with endocytic accessory proteins in the liver cells. After LDL-LDLR complex has been formed, its internalization is promoted by the juxtaposition of ARH to the complex, and by this mechanism LDL fluxes through early endosomes. Therefore, ARH appears to act as a molecular usher, gathering the LDL-LDLR complex into the clathrin-coated vesicles and presumably enhancing the efficiency of vesicle packaging. In hepatocytes of ARH patients, defective function of this sorting adaptor may lead to faulty LDLR traffic and hypercholesterolemia.

Acknowledgments—We thank Helen Hobbs for the kind gift of the anti-ARH and anti-LDLR antibodies. We also thank our colleagues for generously providing important reagents and for helpful suggestions in setting up siRNA experiments.

REFERENCES

1. Brown, M. S., and Goldstein, J. L. (1986) *Science* **232,** 34–47
2. Goldstein, J. L., Hobbs, H. H., and Brown, M. S. (2001) in *The Metabolic and Molecular Bases of Inherited Diseases* (Scriver, C., Beaudet, A., Sly, W., and Valle, D., eds), 8th Ed., pp. 2863–2913, McGraw Hill, New York
3. Goldstein, J. L., Anderson, R. G., and Brown, M. S. (1979) *Nature* **279,** 679–685
4. Pearse, B. M. (1976) *Proc. Natl. Acad. Sci. U. S. A.* **73,** 1255–1259
5. Anderson, R. G., Brown, M. S., and Goldstein, J. L. (1977) *Cell* **10,** 351–364
6. Carpentier, J. L., Gorden, P., Goldstein, J. L., Anderson, R. G., Brown, M. S., and Orci, L. (1979) *Exp. Cell Res.* **121,** 135–142
7. Brown, M. S., Anderson, R. G., and Goldstein, J. L. (1983) *Cell* **32,** 663–667
8. Rudenko, G., Henry, L., Henderson, K., Ichtchenko, K., Brown, M. S., Goldstein, J. L., and Deisenhofer, J. (2002) *Science* **298,** 2353–2358
9. Garcia, C. K., Wilund, K., Arca, M., Zuliani, G., Fellin, R., Maioli, M., Calandra, S., Bertolini, S., Cossu, F., Grishin, N., Barnes, R., Cohen, J. C., and Hobbs, H. H. (2001) *Science* **292,** 1394–1398
10. Zuliani, G., Arca, M., Signore, A., Bader, G., Fazio, S., Chianelli, M., Bellosta, S., Campagna, F., Montali, A., Maioli, M., Pacifico, A., Ricci, G., and Fellin, R. (1999) *Arterioscler. Thromb. Vasc. Biol.* **19,** 802–809
11. Mishra, S. K., Watkins, S. C., and Traub, L. M. (2002) *Proc. Natl. Acad. Sci. U. S. A.* **99,** 16099–16104
12. Arca, M., Zuliani, G., Wilund, K., Campagna, F., Fellin, R., Bertolini, S., Calandra, S., Ricci, G., Glorioso, N., Maioli, M., Pintus, P., Carru, C., Cossu, F., Cohen, J., and Hobbs, H. H. (2002) *Lancet* **359,** 841–847
13. Eden, E. R., Patel, D. D., Sun, X. M., Burden, J. J., Themis, M., Edwards, M., Lee, P., Neuwirth, C., Naoumova, R. P., and Soutar, A. K. (2002) *J. Clin. Investig.* **110,** 1695–1702
14. He, G., Gupta, S., Yi, M., Michaely, P., Hobbs, H. H., and Cohen, J. C. (2002) *J. Biol. Chem.* **277,** 44044–44049
15. Jones, C., Hammer, R. E., Li, W. P., Cohen, J. C., Hobbs, H. H., and Herz, J. (2003) *J. Biol. Chem.* **278,** 29024–29030
16. Cohen, J. C., Kimmel, M., Polanski, A., and Hobbs, H. H. (2003) *Curr. Opin. Lipidol.* **14,** 121–127
17. Pathak, R. K., Yokode, M., Hammer, R. E., Hofmann, S. L., Brown, M. S., Goldstein, J. L., and Anderson, R. G. (1990) *J. Cell Biol.* **111,** 347–359
18. Elbashir, S. M., Harborth, J., Lendeckel, W., Yalcin, A., Weber, K., and Tuschl, T. (2001) *Nature* **411,** 494–498
19. Hinrichsen, L., Harborth, J., Andrees, L., Weber, K., and Ungewickell, E. J. (2003) *J. Biol. Chem.* **278,** 45160–45170
20. van Uzendoom, I. S. C., Zegers, M. M., Kok, J. W., and Hoekstra, D. (1997) *J. Cell Biol.* **137,** 347–357
21. Lian, W. N., Tsai, J. W., Yu, P. M., Wu, T. W., Yang, S. C., Chau, Y. P., and Lin, C. H. (1999) *Hepatology* **30,** 748–760
22. Stockinger, W., Sailler, B., Strasser, V., Recheis, B., Fashing, D., Kahr, L., Schneider, W. J., and Nimpf, J. (2002) *EMBO J.* **16,** 4259–4267
23. Heinonen, J. E., Smith, C. I., and Nore, B. F. (2002) *FEBS Lett.* **527,** 274–278
24. Beisiegel, U., Schneider, W. J., Goldstein, J. L., Andersonm R. G., and Brown, M. S. (1981) *J. Biol. Chem.* **256,** 11923–11931
25. Norman, D., Sun, X. M., Bourbon, M., Knight, B. L., Naoumova, R. P., and Soutar, A. K. (1999) *J. Clin. Investig.* **104,** 619–628
26. Wilund, K. R., Yi, M., Campagna, F., Arca, M., Zuliani, G., Fellin, R., Ho, Y. K., Garcia, J. V., Hobbs, H. H., and Cohen, J. C. (2002) *Hum. Mol. Genet.* **11,** 3019–3030
27. Michaely, P., Li, W. P., Anderson, R. G., Cohen, J. C., and Hobbs, H. H. (2004) *J. Biol. Chem.* **279,** 34023–34031
28. Harada-Shiba, M., Takagi, A., Marutsuka, K., Moriguchi, S., Yagyu, H., Ishibashi, S., Asada, Y., and Yokoyama, S. (2004) *Circ. Res.* **95,** 945–952
29. Carbone, R., Fre, S., Iannolo, G., Belleudi, F., Mancini, P., Pelicci, P. G., Torrisi, M. R., and Di Fiore, P. P. (1997) *Cancer Res.* **57,** 5498–5504
30. Van Dam, A. M., Bol, J. G., Gaykema, R. P., Goehler, L. E., Maier, S. F., Watkins, L. R., and Tilders, F. J. (2000) *Neurosci. Lett.* **285,** 169–172
31. Fouraux, M. A., Deneka, M., Ivan, V., van der Heijden, A., Raymackers, J., van Suylekom, D., van Venrooij, W. J., van der Sluijs, P., and Pruijn, G. J. (2004) *Mol. Biol. Cell* **15,** 611–624
32. Deneka, M., Neeft, M., Popa, I., van Oort, M., Sprong, H., Oorschot, V., Klumperman, J., Schu, P., and van der Sluijs, P. (2003) *EMBO J.* **22,** 2645–2657